JGR Atmospheres

RESEARCH ARTICLE
10.1029/2024JD043117

Assessing Regional Climate Trends in West Africa Under Geoengineering: A Multimodel Comparison of UKESM1 and CESM2

Francis Nkrumah[1], Kwesi A. Quagraine[1,2,3], Gandome Mayeul Leger Davy Quenum[4], Daniele Visioni[5], Hubert A. Koffi[6], and Nana Ama Browne Klutse[6,7]

[1]Department of Physics, University of Cape Coast, Cape Coast, Ghana, [2]NSF National Center for Atmospheric Research, Boulder, CO, USA, [3]Climate System Analysis Group, University of Cape Town, Cape Town, South Africa, [4]University of Abomey-Calavi (UAC), Abomey-Calavi, Benin, [5]Department of Earth and Atmospheric Sciences, Cornell University, Ithaca, NY, USA, [6]Department of Physics, University of Ghana, Accra, Ghana, [7]African Institute of Mathematical Science, Kigali, Rwanda

Key Points:

- SAI could limit global warming but may increase rainfall unpredictability and make extreme weather forecasting more challenging
- SAI can have very different effects depending on the model used
- SAI significantly dampens the warming signal, obscuring detectable trends in precipitation and temperature across much of West Africa

Correspondence to:

K. A. Quagraine,
kwesiq@ucar.edu

Citation:

Nkrumah, F., Quagraine, K. A., Quenum, G. M. L. D., Visioni, D., Koffi, H. A., & Klutse, N. A. B. (2025). Assessing regional climate trends in West Africa under geoengineering: A multimodel comparison of UKESM1 and CESM2. *Journal of Geophysical Research: Atmospheres*, *130*, e2024JD043117. https://doi.org/10.1029/2024JD043117

Received 10 DEC 2024
Accepted 20 JUN 2025

Author Contributions:

Conceptualization: Francis Nkrumah
Data curation: Kwesi A. Quagraine
Formal analysis: Francis Nkrumah
Funding acquisition: Nana Ama Browne Klutse
Supervision: Nana Ama Browne Klutse
Writing – original draft: Francis Nkrumah, Kwesi A. Quagraine
Writing – review & editing: Francis Nkrumah, Kwesi A. Quagraine, Gandome Mayeul Leger Davy Quenum, Daniele Visioni, Hubert A. Koffi, Nana Ama Browne Klutse

Abstract This study investigates West Africa's climate vulnerability under stratospheric aerosol injection (SAI), using UKESM1 and CESM2 models. We analyzed temperature and precipitation responses for 2050–2069 relative to 2015–2034 under SSP2-4.5 and ARISE-SAI-1.5 scenarios. Our approach involved evaluating temperature and precipitation anomalies, applying signal-to-noise ratio (SNR) analysis—defined as the ratio of the forced climate response to internal variability—to assess signal robustness, and using cumulative distribution (CDF) and probability density (PDF) functions to explore shifts in precipitation extremes. Results indicate that under SSP2-4.5, both models project significant warming. UKESM1 simulates increases near 1.8°C, while CESM2 projects between 1.0°C and 1.2°C. Under ARISE-SAI-1.5, UKESM1 shows pronounced cooling, with temperatures dropping up to 0.3°C below the reference period at some latitudes. CESM2 shows a more uniform cooling, with temperatures between 0°C and 0.3°C above the reference. SNR analysis reveals robust, statistically significant temperature changes across the region, clearly emerging above natural variability by midcentury. Precipitation changes, however, show lower SNR values and greater spatial uncertainty, suggesting weaker and less predictable hydrological responses. CDF and PDF analyses highlight complex shifts in precipitation extremes, suggesting that while SAI could counteract warming trends, it may introduce additional variability and uncertainty in rainfall projections. These results emphasize the importance of multimodel comparisons in assessing geoengineering impacts on regional climates, as differing sensitivities to radiative forcing and feedback can produce divergent outcomes.

Plain Language Summary This study explores how stratospheric aerosol injection (SAI) could impact West Africa's climate using two models, UKESM1 and CESM2. Between 2050 and 2069, without SAI, both models project significant warming, with UKESM1 showing larger increases (1.8°C) than CESM2 (1.0–1.2°C). Under SAI, UKESM1 predicts notable cooling, even below baseline levels, while CESM2 shows milder effects. Rainfall extremes respond unpredictably, with increased variability under SAI. Although SAI may reduce warming, it introduces uncertainty, especially for precipitation. These findings highlight the importance of using multiple models to understand the complex impacts of geoengineering on vulnerable regions like West Africa.

1. Introduction

West Africa faces severe vulnerability to climate change, particularly through shifting rainfall patterns and rising temperatures. According to recent projections, the Sahel region is expected to experience a temperature increase of approximately 2°C by 2050 under the Shared Socioeconomic Pathway 2–4.5 (SSP2-4.5) scenario (Limantol et al., 2023; Richter et al., 2022). This regional vulnerability is underscored by global efforts to limit warming to 1.5°C as agreed under the Paris Agreement (UNFCCC, 2015), highlighting the urgency of exploring all mitigation and intervention strategies. The Guinea Coast has been observed to experience warming, with mean annual temperatures rising by 1.0–1.5°C (IPCC, 2021). These warming trends, combined with increasingly erratic rainfall, present significant challenges to the region's agricultural productivity and food security. Smallholder farmers, who rely heavily on rain-fed agriculture, are particularly at risk from the combination of higher temperatures and unpredictable rainfall patterns (Klutse et al., 2021; MacCarthy et al., 2021), a challenge echoed in

global assessments (IPCC, 2021). A recent synthesis indicates that crop yields in West Africa could decline by a median of 6% due to these climatic shifts (Ahmed et al., 2015; Carr et al., 2022), consistent with observed sensitivities of agriculture to monsoon variability (Sultan et al., 2019).

Climate projections indicate an increasing threat of more frequent and severe droughts across West Africa, intensifying water stress throughout the region (Akumaga & Tarhule, 2018). The rising occurrence of extreme weather events—such as floods and heatwaves—poses multiple challenges: disrupting agricultural cycles, straining water resources, and overwhelming both infrastructure and public health systems (Muzammal et al., 2024; Onyeaka et al., 2024; Sivakumar, 2020). The vulnerability of the region's food systems is particularly concerning. With 90%–95% of African food production depending on rainfall, food insecurity is one of the continent's most significant climate-related risks (Fao, 2018; Sultan & Gaetani, 2016). The potential for severe resource conflicts among competing interest groups underscores the complex socioeconomic implications of climate change in the region (Fraumeni & Liu, 2021). Given these challenges, there is an urgent need for comprehensive adaptation strategies that address not only environmental concerns but also social, economic, and political dimensions to ultimately strengthen the resilience of West African communities.

In response to these pressing challenges, researchers are exploring innovative solutions to offset climate impacts with stratospheric aerosol injection (SAI), emerging as one potential approach. SAI is a geoengineering method that proposes artificially cooling the Earth's surface by introducing reflective particles into the stratosphere, thereby increasing the planet's albedo and reducing incoming solar radiation (Irvine et al., 2019; Smith et al., 2022). The Intergovernmental Panel on Climate Change (IPCC) has recognized SAI as a potential strategy to limit global temperature increases (IPCC, 2021). Foundational research has demonstrated SAI's potential effectiveness, with modeling experiments suggesting that large-scale implementation could lower global surface temperatures by several degrees (Kravitz et al., 2017; Robock et al., 2008). Various deployment scenarios have been proposed to evaluate the climate response under different strategies (MacMartin et al., 2022). However, these studies also caution against potential unintended consequences, such as disruptions to regional climate patterns, changes in precipitation, and impacts on ecosystems and agriculture in Africa (Obahoundje et al., 2022; Patel et al., 2023; Tilmes et al., 2018). This concern is particularly relevant for West Africa, where the monsoon system determines rainfall patterns and agricultural productivity. The West African Monsoon (WAM) is a critical component of the region's climate system, typically occurring from June to September. According to Atiah et al. (2021), the monsoon season has experienced increased variability in recent decades, with a tendency toward later onset and earlier cessation. Nicholson et al. (2018) reported that the monsoon duration has decreased by approximately 5–10 days over the past 30 years, particularly in the Sahel region. This shortening of the monsoon season has important implications for rain-fed agriculture and food security in West Africa. Modeling studies, such as those conducted by Jones et al. (2018), suggest that SAI could potentially alter monsoon circulation patterns and precipitation distribution across West Africa. The sensitivity of the WAM to changes in atmospheric circulation and moisture transport highlights the need for comprehensive research on SAI's potential side effects on regional climate systems.

Beyond the biophysical impacts, it is important to consider the socioeconomic and ethical implications of deploying SAI in West Africa. The region's economies and food security depend on predictable rainfall and temperature regimes; disruptions to the monsoon could affect millions of livelihoods. Moreover, West African nations contribute less than 4% of global greenhouse gas emissions, yet they could disproportionately bear the risks (or benefits) of any global-scale climate intervention (Shindell et al., 2023). This imbalance raises questions of climate justice and underscores the need for inclusive governance frameworks for SAI. In practice, any discussion of implementing SAI would need to ensure that African stakeholders have a seat at the table and that potential regional consequences are carefully managed. These considerations provide crucial context for interpreting the model results presented in this study.

This study aims to comprehensively assess regional climate trends in West Africa using specific SAI geoengineering strategies. Specifically, we will

1. Assess how SAI strategies under the "Assessing Responses and Impacts of Solar Climate Intervention on the Earth with Stratospheric Aerosol Injection" (ARISE-SAI-1.5) (Richter et al., 2022) scenario could alter temperature and precipitation patterns in West Africa (both the Sahel and Guinea Coast regions).
2. Evaluate the implications of these changes for regional agricultural productivity and water resource management.

To achieve these objectives, we employ two advanced climate models: UKESM1 (Sellar et al., 2019) and CESM2 (Danabasoglu et al., 2020; Gettelman et al., 2019). These models were selected for their ability to effectively run ARISE-SAI-1.5 simulations under the same greenhouse gas emission scenario, specifically the SSP2-4.5 pathway. Additionally, both models utilize a consistent multitarget, multilatitude SAI strategy, allowing for a reliable comparison of their outputs regarding regional climate impacts at a monthly mean timescale. This approach facilitates identifying consistencies and discrepancies between models, highlighting areas of high confidence in projections and those requiring further investigation. Given West Africa's vulnerability to climate change and its potential sensitivity to geoengineering interventions, this study's findings are crucial for informing future climate adaptation and strategies to offset regional warming impacts.

2. Data and Methodology

This study employs two advanced Earth System Models (ESMs)—the UK Earth System Model (UKESM1) and the Community Earth System Model version 2 (CESM2)—to assess the impact of stratospheric aerosol injection (SAI) on temperature and precipitation in West Africa. UKESM1 integrates the HadGEM3-GC3.1 model, which encompasses the physical atmosphere-land-ocean-sea ice system with a horizontal resolution of 1.875° × 1.25° and 85 vertical levels, alongside the United Kingdom Chemistry and Aerosol (UKCA) model for detailed atmospheric chemistry simulations (Sellar et al., 2019). In contrast, CESM2 utilizes the Whole Atmosphere Community Climate Model (WACCM6) as its atmospheric component, featuring a finer horizontal resolution of 1.25° × 0.9° and extending to 140 km with 70 vertical levels (Gettelman et al., 2019). Both models include sophisticated aerosol-cloud interaction schemes, which are essential for evaluating the impacts of SAI on regional climate patterns (Richter et al., 2022).

UKESM1 and CESM2 have noteworthy differences in their treatment of aerosols, radiation, and clouds. UKESM1 includes the UKCA module, which allows the interactive simulation of stratospheric sulfate aerosol formation and its radiative effects, whereas CESM2 (WACCM6) uses the MAM4 aerosol scheme with specified SO_2 injections. The models also employ different atmospheric physics packages: for example, UKESM1 uses the GA7.1 configuration (Walters et al., 2019) with the SOCRATES radiative transfer model, while CESM2 uses the RRTMG radiation scheme (Gettelman et al., 2019). Furthermore, their cloud microphysics and convective parameterizations differ (e.g., UKESM1's prognostic cloud fraction vs. CESM2's Zhang-McFarlane convection), which can influence how each model translates aerosol forcing into cloud and precipitation responses. We chose these two models because both were able to run the identical ARISE-SAI-1.5 scenario under a common SSP2-4.5 baseline, and their contrasting process representations provide a robust test of result sensitivity to model formulation.

To analyze the effects of SAI, the study uses the Shared Socioeconomic Pathway 2–4.5 (SSP2-4.5) as the baseline, representing an intermediate mitigation scenario (O'Neill et al., 2016) without any aerosol injections. The baseline SSP2-4.5 simulations begin in 2015 and run until 2100. By using the same emissions scenario and SAI strategy for both models, we ensure that any differences in outcomes can be attributed to model response differences rather than experimental setup.

From 2035 to 2070, both models simulate the SAI under the Assessing Responses and Impacts of Solar Climate Intervention of the Earth System-SAI (ARISE-SAI-1.5) scenario. This scenario aims to maintain global mean temperatures at 1.5 K above preindustrial levels, in line with international climate threshold (MacMartin et al., 2022) and one of the Paris COP21 agreements. The scenario builds on previous geoengineering design studies (Kravitz et al., 2017) to maintain a specified temperature trajectory. Starting in the year 2035, SO_2 was injected at four equatorial and subtropical locations (15°N, 15°S, 30°N, 30°S, at ~21 km altitude) each year, with injection amounts dynamically adjusted via a feedback control algorithm to achieve the temperature goal (Ritcher et al., 2022). This multilatitude approach was designed to balance both interhemispheric and equator-to-pole temperature gradients, addressing potential regional differences in the effects of tropical-only SAI.

Multiple ensemble members were employed for each model to enhance the robustness of the results. The CESM2 model includes 10 ensemble members, whereas UKESM1 uses five. The difference in the ensemble members is due to data availability. Although the CESM2 ensemble comprises 10 members, only five UKESM1 members from the ARISE-SAI-1.5 experiment were available with consistent variables. This approach facilitates inter-model comparisons and improves the statistical reliability of SAI-induced anomaly detection. By incorporating ensemble simulations, this study accounted for internal climate variability and provided a more comprehensive

assessment of the potential outcomes of SAI implementation. For consistency in the analysis across models, the outputs were regridded to a common spatial resolution. This standardization process is crucial for comparing results from different models with varying native resolutions. This also enables a more accurate assessment of regional climate impacts, particularly in West Africa, where local-scale variations can significantly influence the temperature and precipitation patterns.

This study evaluated the impact of stratospheric aerosol injection (SAI) on the near-surface air temperature and precipitation rates in West Africa. The study analyzed monthly output from the UKESM1 and CESM2 climate models. For temperature, we derived annual and seasonal means of monthly near-surface air temperature. For precipitation, we used monthly total precipitation, which was aggregated into annual and seasonal averages. It focused on the region between 4°N–24°N and 18°W–18°E, calculating anomalies for the period 2050–2069 relative to a reference period from 2015 to 2034 for each model. The analysis included an examination of temporal trends in the annual mean and seasonal temperature and precipitation, with results decomposed by seasons to assess potential impacts on West Africa's monsoon cycle and the dry season. This seasonal analysis is critical for evaluating the possible consequences on agriculture, water resources, and overall ecosystem functioning in West Africa, where the monsoon plays a vital role in sustaining livelihoods and biodiversity.

The period 2050–2069 was chosen for this comparative analysis to align with midcentury climate projections under the Shared Socioeconomic Pathway 2–4.5 (SSP2-4.5), which provides an appropriate timeframe for assessing the impacts of the ARISE-SAI-1.5 geoengineering strategy. This timeframe allows for a detailed examination of the models' responses to geoengineering interventions against a backdrop of intermediate greenhouse gas emissions. Furthermore, it coincides with critical junctures in West Africa's climate dynamics and agricultural cycles, providing valuable insights into the region's adaptation needs and the potential role of geoengineering in offsetting adverse climate impacts. This comparative analysis thus serves as a vital tool for understanding the effectiveness, risks, and uncertainties associated with implementing SAI in a region highly vulnerable to climate change.

To further analyze the coupled responses of temperature and precipitation over West Africa, scatterplots were constructed comparing changes in mean surface temperature (ΔTs) and precipitation (ΔPr) for the period 2050–2069 relative to the reference period (2015–2034).

ΔTs were computed as the difference between the multiensemble mean surface air temperature during the future period (2050–2069) and that of the reference period (2015–2034) at each grid point, averaged over the defined West African domain (18°W–18°E, 4°N–24°N). Similarly, ΔPr was calculated as the difference between future and reference period mean precipitation rates, expressed in millimeters per day (mm/day), averaged over the same spatial domain. Separate calculations were performed for each model (UKESM1 and CESM2) and each scenario (SSP2-4.5 and ARISE-SAI-1.5).

To quantify the strength and reliability of the simulated SAI effects on temperature and precipitation in West Africa, a signal-to-noise ratio (SNR) analysis was conducted following a reference-based approach. First, the SNR for SSP2-4.5 alone was calculated at each grid point as the difference between the ensemble mean of the future period (either 2035–2054 or 2050–2069) and the reference period, divided by the ensemble mean standard deviation during the reference period. This formulation evaluates the emergence of the forced climate signal under greenhouse gas emissions relative to natural variability. Second, the intervention-based SNR was computed to quantify the additional effect of solar aerosol injection by calculating the difference between the ARISE-SAI-1.5 future anomaly and the SSP2-4.5 future anomaly, normalized by the reference-period variability. In this case, anomalies were defined relative to the 2015–2034 SSP2-4.5 mean to ensure consistency across scenarios. This method ensures that the SNR accurately captures the forced signal relative to the background climate noise, following practices recommended by Hawkins and Sutton (2009). An SNR greater than +1 indicates a robust and detectable warming (or wetting) signal, while an SNR less than −1 indicates a detectable cooling (or drying) signal. SNR magnitudes between −1 and +1 suggest that projected changes are comparable to internal variability and thus less confidently detectable.

To assess the statistical significance of temperature and precipitation anomalies, we applied different tests based on the distribution of the data. For temperature anomalies, we used the Student's *t*-test, a parametric test that assumes normally distributed data, to determine whether the differences between the future and reference periods were statistically significant. Similarly, for precipitation anomalies that followed a Gaussian distribution, we also

applied the *t*-test to evaluate significance. However, given that precipitation data often exhibit non-Gaussian characteristics due to skewness and extreme values, we first conducted the D'Agostino-Pearson normality test to assess whether the precipitation anomalies conformed to a normal distribution. If the test indicated a non-Gaussian distribution, we applied the Mann-Whitney *U* test, a nonparametric test that does not assume normality. This approach ensured that statistical testing was appropriately tailored to the nature of the data, providing a more robust evaluation of significant climate anomalies. Statistical significance was assessed at each grid point between SAI and SSP2-4.5 ensemble members during 2050–2069. Regions where the differences are statistically significant at the 95% confidence level ($p < 0.05$) were identified through stippling.

The study also examined the annual mean ΔPr as a function of temperature change for both models under the SAI and SSP2-4.5 scenarios relative to their reference periods. This analysis aimed to ascertain the impact of SAI on the hydrological cycle in West Africa. By investigating the relationship between temperature and precipitation changes, researchers could gain insights into how SAI might affect a region's water resources and climate patterns.

To further assess the shifts in the probability distributions of temperature and precipitation under SAI compared to baseline conditions, the cumulative distribution function (CDF) was employed. This statistical tool allows for evaluating the likelihood of extreme climate events under different climate intervention scenarios. By comparing the CDFs for the SAI and SSP2-4.5 scenarios, researchers could identify potential changes in the frequency and intensity of extreme weather events in West Africa.

Additionally, the probability density function (PDF) was used to examine the distribution shapes of the temperature and precipitation anomalies under SAI. This analysis provides insights into shifts in the central tendency, spread, and skewness resulting from SAI interventions. By comparing PDFs, researchers could identify subtle changes in the distribution of temperature and precipitation patterns that might not be apparent from simple averages or trend analyses.

The cumulative distribution functions (CDFs) and probability density functions (PDFs) were constructed from the absolute monthly precipitation and temperature values (not anomalies). For each model and scenario, we aggregated the 20 years (2050–2069) into a single distribution of monthly values across West Africa. This allows a direct assessment of how the overall distribution shifts under SAI compared to the SSP2-4.5 baseline.

The comprehensive approach employed in this study, which combines multiple statistical tools and analyses, allows for a thorough examination of the potential impacts of SAI on West Africa's climate. By considering both temperature and precipitation changes and their interactions and distributions, this study provides valuable insights into the complex effects of climate intervention strategies on regional climate patterns. This information is crucial for policymakers and scientists working to address climate change and its impact on vulnerable regions such as West Africa.

3. Results and Discussion

3.1. Temporal Trends in Temperature and Precipitation

Figure 1 shows the mean near-surface air temperature over West Africa for all simulations of the reference scenario (SSP2-4.5 in red) and the ARISE-SAI-1.5 scenario (blue). Temperature projections under the SSP2-4.5 scenario show a consistent warming trend, increasing steadily after 2020 and approaching 2.0 K by 2070 (Figure 1a). In contrast, the ARISE-SAI-1.5 simulations using the UKESM1 model demonstrate a significant cooling effect, with temperatures decreasing after 2040, coinciding with the onset of the SAI deployment (around 2035), and remaining below the baseline (0 K anomalies) throughout the 2050s and 2060s. This sudden cooling is likely due to the rapid injection of aerosols reaching an effective concentration, leading to a strong transient radiative forcing. This finding aligns with existing literature that suggests SAI could effectively counter warming trends when implemented at optimal latitudes (Henry et al., 2023; MacMartin et al., 2022; Zhang et al., 2024). The UKESM1 model results indicate some internal variabilities, particularly in later decades, as indicated by the spread of the blue lines across ensemble members. These variabilities are consistent with findings from other studies that highlight diverse model responses to aerosol forcing (e.g., Richter et al., 2022).

The ARISE-SAI-1.5 simulation using CESM2 demonstrates a cooling effect relative to the reference SSP2-4.5 scenario, though it is notably less pronounced than in UKESM1 (Figure 1b). After 2040, temperatures remain

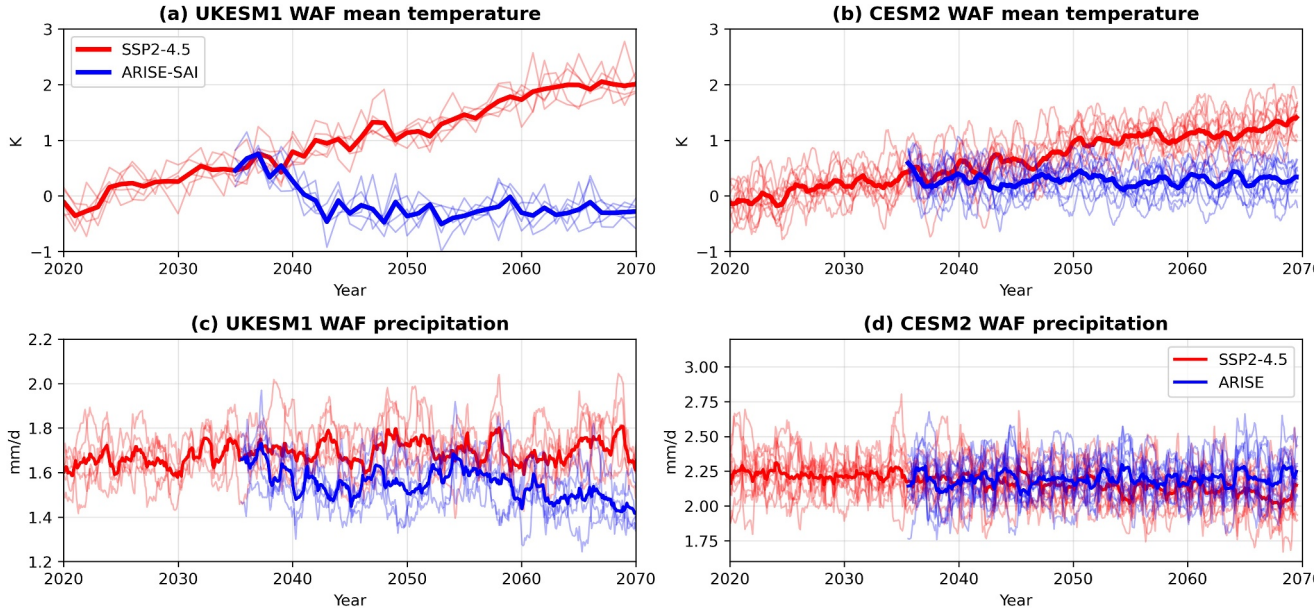

Figure 1. Projected changes in West African regional mean (a, b) near-surface air temperature and (c, d) precipitation under the SSP2-4.5 scenario (red lines) and the ARISE-SAI-1.5 scenario (blue lines) from 2020 to 2070. Panels (a, c) show UKESM1 results; panels (b, d) show CESM2 results. Thin lines represent individual ensemble members, while thick lines are the ensemble means. All values represent spatial averages over the West African domain bounded by 4°N–24°N latitude and 18°W–18°E longitude.

fairly close to the 0 K baseline, with significant variation among ensemble members suggesting greater uncertainty in CESM2's simulation of SAI impacts. This model-to-model difference likely stems from their distinct representations of aerosol-cloud interactions and stratospheric processes (Bednarz et al., 2023). UKESM1 exhibits a more robust response to aerosol forcing, producing consistent and sustained cooling effects, whereas CESM2 shows greater variability in its responses (Henry et al., 2023).

The SAI-induced cooling becomes evident around 2040 in both models; however, UKESM1 exhibits a more abrupt ΔT. There is a notable overlap between the SSP2-4.5 and ARISE-SAI trajectories in the early 2040s, indicating differences in how each model handles the timing and strength of SAI's impact on radiative forcing. Previous research has indicated that such discrepancies can arise from variations in model parameterizations and feedback mechanisms (Fasullo & Richter, 2023). For example, studies have shown that different injection strategies can lead to varying impacts on regional climate systems due to their effects on atmospheric circulation and temperature gradients (Tilmes et al., 2018; Visioni et al., 2023).

A comparative analysis of precipitation responses between UKESM1 and CESM2 models from 2020 to 2070 reveals distinct patterns under SSP2-4.5 and ARISE-SAI scenarios in West Africa. The UKESM1 model under the SSP2-4.5 scenario shows a relatively stable precipitation pattern averaging 1.6 mm/day throughout the period, with some interannual variability (Figure 1c). In contrast, the ARISE-SAI scenario depicts a different trajectory with precipitation decreasing gradually around the year 2040, with a notable decrease between 2040 and 2060, as shown by the ensemble mean consistently dropping below the SSP2-4.5 line. This precipitation reduction suggests that SAI could adversely impact regional hydrological cycles, potentially reducing rainfall in climate-sensitive regions like West Africa. These findings align with previous studies demonstrating that SAI could alter precipitation patterns by influencing atmospheric circulation and moisture transport mechanisms (Tilmes et al., 2013).

CESM2's precipitation projections under the SSP2-4.5 scenario demonstrate a stable pattern, though with a notably higher baseline of approximately 2.25 mm/day compared to UKESM1's 1.6 mm/day (Figure 1d). A key distinction emerges in CESM2's response to SAI: unlike UKESM1's marked precipitation decrease, CESM2 shows minimal difference between its SSP2-4.5 and ARISE-SAI scenarios. This reduced sensitivity to SAI aligns with Fasullo and Richter's (2023) research, which attributes CESM2's muted precipitation response to its distinct handling of aerosol-cloud interactions compared to other climate models.

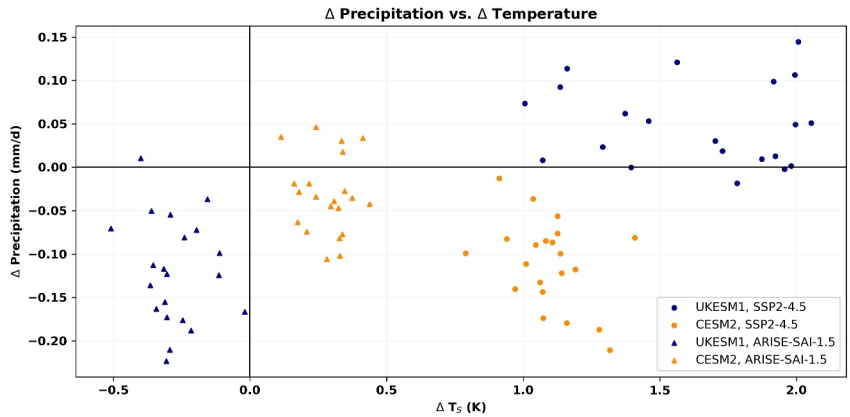

Figure 2. Comparison of the annual mean precipitation change as a function of temperature change for UKESM1 (blue) and CESM2 (yellow) models under the SSP2-4.5 simulations (circle) and the ARISE-SAI-1.5 simulations (triangle).

The relationship between changes in precipitation (Δ Precipitation) and temperature (Δ Temperature) for both models reveals further insights (Figure 2). In UKESM1's SSP2-4.5 scenario, rising temperatures correlate with modest precipitation increases, though with notable variability—a finding that aligns with previous research showing enhanced evaporation and precipitation in warmer conditions, as discussed in Trenberth and Shea (2005). Conversely, CESM2 shows a different response where increasing temperatures correlate with a gradual decrease in precipitation, indicating a drier future for West Africa under warming conditions compared to UKESM1. These differences reflect structural contrasts in the models. UKESM1 incorporates more active aerosol-cloud interactions and stronger hydrological feedbacks that sustain or enhance monsoon rainfall. CESM2, in contrast, features a more conservative convection scheme and weaker aerosol forcing, leading to a drying signal and a southward shift in rainfall patterns. Similar differences in Sahel rainfall responses between these models have been documented in recent studies (Gettelman et al., 2019; Sellar et al., 2019).

For the ARISE-SAI scenario, UKESM1 demonstrates a consistent relationship between changes in temperature and precipitation: as temperatures decrease due to the cooling effect of SAI, precipitation also tends to decline, especially during larger negative temperature anomalies (Figure 2). This finding is supported by studies suggesting that SAI-induced cooling does not return the hydrological cycles to their previous target state completely (Visioni et al., 2023). In contrast, CESM2 exhibits a more scattered relationship where decreasing temperatures under SAI correlate with reduced precipitation; however, some instances show little to no ΔPr despite cooling. This variability in CESM2 projections suggests that SAI's influence on regional precipitation patterns may be more nuanced and geographically dependent than initially anticipated.

3.2. Spatial Patterns of Temperature and Precipitation Change

The projected near-surface air temperature changes for West Africa during 2050–2069 reveal distinct patterns across models and scenarios (Figure 3). The UKESM1 model under the SSP2-4.5 scenario shows a clear warming trend across the region, with temperature increases ranging from 0.7 to 2.4 K relative to the reference period. The highest warming is concentrated in the Sahel region (north of 12°N), while the Guinea Coast experiences milder increases, showing geographical variations. These projections are consistent with existing literature, highlighting stronger warming in arid and semiarid regions like the Sahel (Richter et al., 2022; Tebaldi et al., 2021).

The CESM2 model exhibits a warming pattern similar to UKESM1, though with more uniform temperature increases across the region, showing variations between 0.7 and 1.7°C. A key distinction emerges in the northern Sahel, where CESM2 projects less intense warming compared to UKESM1. This variation between the models likely stems from their different approaches to parameterization and regional climate dynamics simulation, as noted by Henry et al. (2023).

Under the ARISE-SAI scenario, UKESM1 exhibits pronounced cooling effects, with temperature reductions between 0 and −1.4°C across most regions compared to the reference period. The Sahel experiences vast cooling, although not significant, particularly north of 12°N, where temperatures drop by over 0.5°C with respect to the

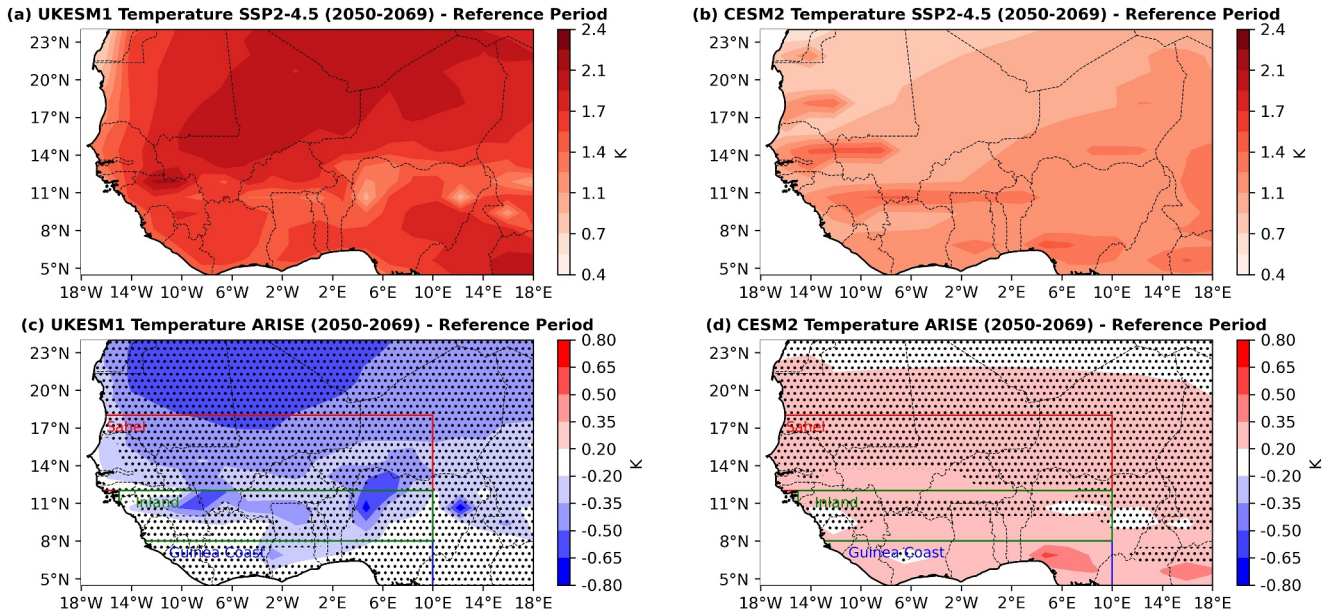

Figure 3. Annual-mean and ensemble-mean near-surface temperature anomalies (K) for the 2050–2069 period relative to the reference period (2015–2034) for UKESM1 and CESM2 under the SSP2-4.5 and ARISE-SAI-1.5 scenarios. Panels (a) and (b) show spatial temperature anomalies under SSP2-4.5; panels (c, d) show the anomaly under ARISE-SAI-1.5. Stippled regions indicate nonstatistically significant changes relative to the reference period (two-sided *t*-test, $p < 0.05$). Panels (c, d) also illustrate the subregional divisions used for zonal analysis: Sahel (12°–18°N), Inland (8°–12°N), and Guinea Coast (4°–8°N), spanning 18°W to 18°E.

reference period. This dramatic cooling illustrates how SAI could effectively counteract some of the warming effects of climate change, especially in sensitive regions like the Sahel. Previous research supports this notion that SAI could significantly offset temperature increases by reflecting solar radiation into space (Kravitz et al., 2017; Tilmes et al., 2018). The temperature response under both scenarios differs regionally, with the Sahel experiencing widespread changes in warming (SSP2-4.5) and cooling (ARISE-SAI) compared to the Inland and Guinea Coast regions. This suggests that the Sahel may be more sensitive to climate change and geoengineering interventions. It is noteworthy that cooling under ARISE-SAI in the Inland region tends to be statistically significant than in the Sahel.

In contrast, CESM2 under the ARISE-SAI scenario shows a general cooling trend across West Africa relative to the baseline climate; however, some areas, such as the Guinea Coast, exhibit minimal or no deviation from baseline temperatures. This suggests that while SAI may partially offset warming, its effectiveness in restoring preintervention climate conditions is spatially heterogeneous (Visioni et al., 2023).

This suggests that UKESM1's effective climate sensitivity or regional feedbacks are larger. When SAI is applied, UKESM1's higher sensitivity yields a larger temperature reduction, even overcooling some areas, whereas CESM2's lower sensitivity yields a milder response. Additionally, model-specific feedback processes likely play a role: UKESM1 may have stronger cooling feedback (e.g., more low cloud formation or higher aerosol optical depth in the tropics), amplifying regional cooling. In contrast, CESM2 might distribute the aerosol cooling more evenly or counteract it slightly via its climate feedbacks, resulting in less cooling in West Africa. Previous intermodel studies have noted such differences—the same SAI strategy can produce varying tropical cooling due to model physics (Henry et al., 2023).

Since annual mean precipitation changes may mask important seasonal variations, this analysis also focuses on seasonal precipitation changes to better capture intraannual variability and regional differences. Figure 4 illustrates the precipitation anomalies for West Africa during the 2050–2069 period compared to their respective reference periods under the SSP2-4.5 and ARISE-SAI-1.5 scenarios, specifically examining seasonal responses from both UKESM1 and CESM2 models. The analysis distinguishes between the dry season (DJF–December, January, February) and the wet season (JJA–June, July, August). Shaded areas in the figure indicate regions where differences are not statistically significant, as assessed using a two-sided *t*-test with a significance level of $p < 0.05$, considering all ensemble members and treating the 20 years as independent samples.

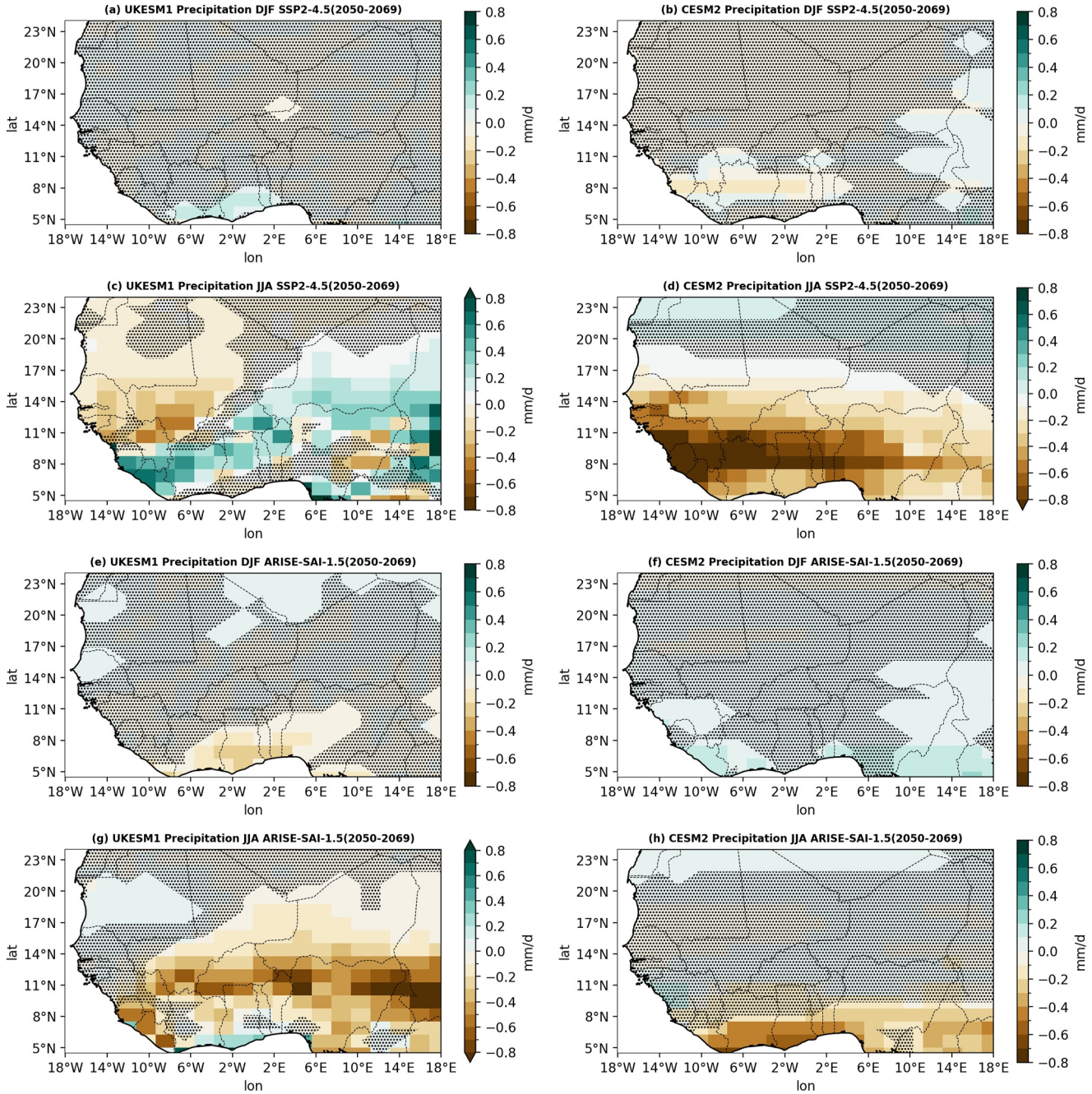

Figure 4. Comparison of ensemble-mean seasonal precipitation change from 2050 to 2069 for UKESM1 and CESM2, for SSP2-4.5 and ARISE-SAI-1.5, and DJF and JJA, relative to the reference period mean (2015–2034). DJF refers to December, January, and February, and JJA refers to June, July, and August. Stippled areas indicate where the difference is not statistically significant, as evaluated using a double-sided *t*-test with $p < 0.05$, considering all ensemble members as independent samples.

In the December–January–February (DJF) season, UKESM1 under the SSP2-4.5 scenario predicts slight increases in precipitation across southern West Africa relative to the reference period, particularly around the Guinea Coast (Figure 4a). However, northern regions of the Sahel experience minimal or slightly negative changes in precipitation, with many areas showing no statistically significant variation. This indicates that while SSP2-4.5 may lead to wetter conditions in coastal regions, it does not significantly alter precipitation patterns further north. In contrast, CESM2 projects widespread drying across much of West Africa during DJF, especially in the Sahel, with significant reductions projected in central West Africa extending into parts of the Guinea Coast (Figure 4b).

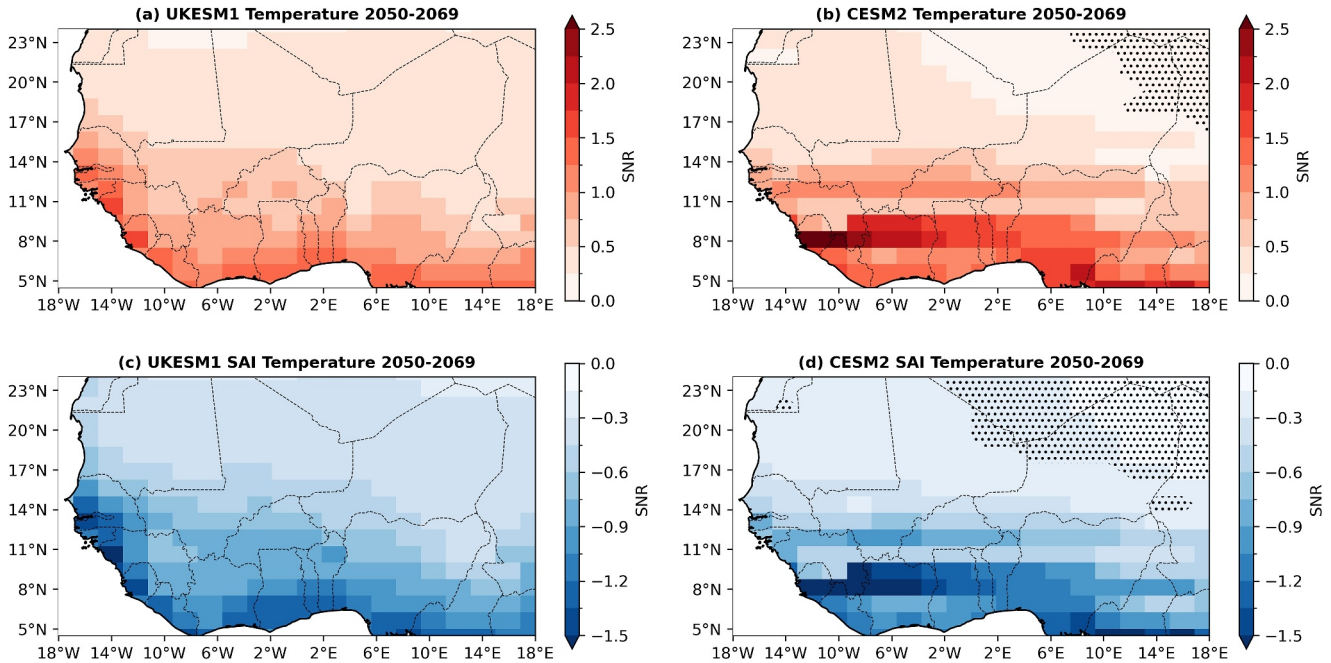

Figure 5. Spatial distribution of signal-to-noise ratio (SNR) of surface air temperature anomalies over West Africa during 2050–2069, relative to the reference period (2015–2034). Panels (a, b) show the SNR under SSP2-4.5 for the UKESM1 and CESM2 models, respectively, while panels (c, d) present the SNR under the ARISE-SAI-1.5 scenario. Stippling denotes grid points where differences are not statistically significant at the 95% confidence level ($p < 0.05$).

During the June–July–August (JJA) season, UKESM1 displays a mixed precipitation response, with notable increases along the Guinea Coast and central Sahel regions, although decreases are evident in the western inland Sahel (Figure 4c). Statistically significant areas are mainly projected to occur in regions of increased precipitation near the Guinea Coast. Conversely, CESM2 exhibits a much stronger drying trend across both the Sahel and Guinea Coast during JJA (Figure 4d), with losses exceeding 0.4 mm/day in core monsoon regions. This pattern reflects CESM2's more conservative convective dynamics and weaker moisture recycling.

Under the ARISE-SAI-1.5 geoengineering scenario, both models demonstrate reductions in precipitation compared to SSP2-4.5, but spatial patterns differ significantly. In DJF (Figure 4e), UKESM1 shows significant drying along the Guinea Coast, while CESM2 (Figure 4f) indicates statistically significant wetting across much of the Sahel and Guinea Coast, suggesting that SAI alleviates dry conditions in these areas compared to SSP2-4.5. In JJA, UKESM1 projects strong drying along the Guinea Coast and Inland areas (Figure 4g), likely reflecting SAI's cooling effect that limits convection and suppresses monsoonal rainfall, consistent with findings on SAI's impacts on monsoon regions (Niemeier et al., 2020). In contrast, CESM2 shows less severe drying during JJA under ARISE-SAI-1.5, with some areas demonstrating no distinguishable changes from the baseline climate (Figure 4h).

Our regional findings for West Africa align with several global-scale results reported by Henry et al. (2023), particularly in terms of model differences, spatial response patterns, and climate trade-offs under SAI. Both UKESM1 and CESM2 achieved substantial cooling under ARISE-SAI-1.5, yet UKESM1 exhibited stronger temperature reductions due to its smaller aerosol particle size and higher optical depth, reflecting greater cooling efficiency per unit sulfur injected. This mirrors Henry et al.'s global results, where UKESM1 produced more pronounced cooling but also stronger suppression of precipitation, particularly in the tropics. Regionally, we found that SAI helped preserve Sahel rainfall while enhancing drying along the Guinea Coast; a pattern consistent with Henry et al.'s observation that SAI tends to reduce equatorial convection more than subtropical rainfall.

3.3. Signal-To-Noise Ratio (SNR) Analysis for Robustness

Figure 5 shows the spatial distribution of the signal-to-noise ratio (SNR) for surface air temperature anomalies over West Africa for 2050–2069, relative to the reference period, with stippling denoting regions where the signal

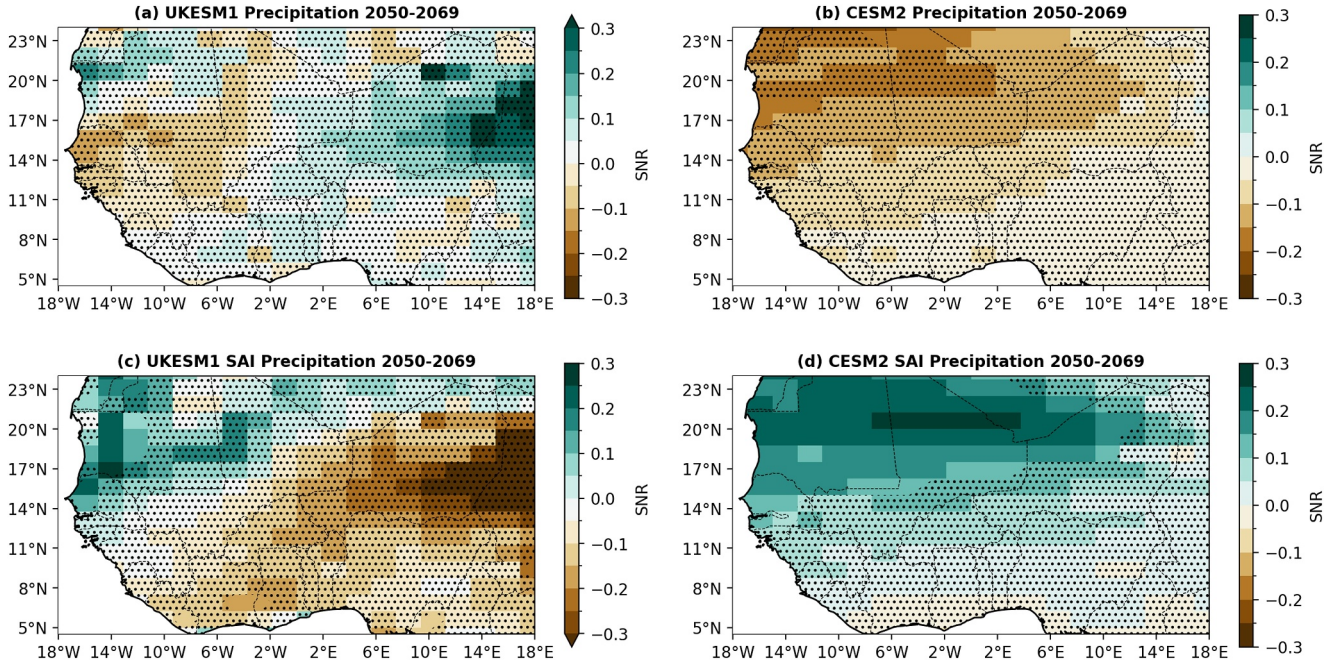

Figure 6. Spatial distribution of signal-to-noise ratio (SNR) of precipitation anomalies over West Africa during 2050–2069, relative to the reference period (2015–2034). Panels (a, b) show the SNR under SSP2-4.5 for the UKESM1 and CESM2 models, respectively, while panels (c, d) present the SNR under the ARISE-SAI-1.5 scenario. Stippling denotes grid points where differences are not statistically significant at the 95% confidence level ($p < 0.05$).

is not statistically significant at the 95% confidence level ($p \geq 0.05$). Areas without stippling represent locations where the projected climate signals are highly certain.

Under SSP2-4.5 (Figures 5a and 5b), both UKESM1 and CESM2 project strong and statistically significant warming across most of West Africa, as indicated by positive SNR values and the absence of stippling over large parts of the domain. The most robust warming signals are located south of approximately 15°N, where SNR values exceed 1.0. However, the north-eastern parts of the domain, especially in CESM2 (Figure 5b), highlight areas where warming signals are weaker relative to internal variability, leading to reduced statistical confidence in those zones. These areas of nonsignificant warming may reflect either higher natural climate variability.

In the ARISE-SAI-1.5 scenario (Figures 5c and 5d), widespread and significant cooling signals are evident over much of West Africa, particularly south of 15°N, where negative SNR values (down to −1.6) dominate. This indicates that geoengineering deployment would produce a statistically detectable cooling effect across these regions. Nevertheless, in parts of northern West Africa, especially in CESM2 (Figure 5d), cooling signals are less robust, likely due to spatial variability in aerosol effects. These areas of nonsignificance imply greater uncertainty in the effectiveness of SAI in stabilizing temperatures at higher latitudes within the region.

Overall, the results demonstrate that climate change signals under SSP2-4.5 and ARISE-SAI-1.5 are detectable against internal variability and statistically significant across most of West Africa by midcentury, especially in the monsoon-influenced southern belt. However, the presence of nonsignificant areas, particularly in the northern margins, underscores the importance of localized assessments when considering regional climate interventions. Understanding robust and uncertain zones is critical for informing targeted adaptation strategies under future climate change or geoengineering scenarios.

The SNR analysis of precipitation over West Africa during the period 2050–2069, relative to the reference period, provides key insights into the reliability of precipitation projections under different scenarios (Figure 6). Across both models and scenarios, the precipitation SNR values are generally low, predominantly ranging between −0.3 and +0.3. This indicates that projected precipitation changes are small relative to the internal variability of the reference period. Under SSP2-4.5 (Figures 6a and 6b), positive SNR values (wetting signals) and negative SNR values (drying signals) are scattered across the region, but regions without stippling are sparse, highlighting that only limited areas show statistically robust changes. In UKESM1 (Figure 6a), the precipitation signal is highly

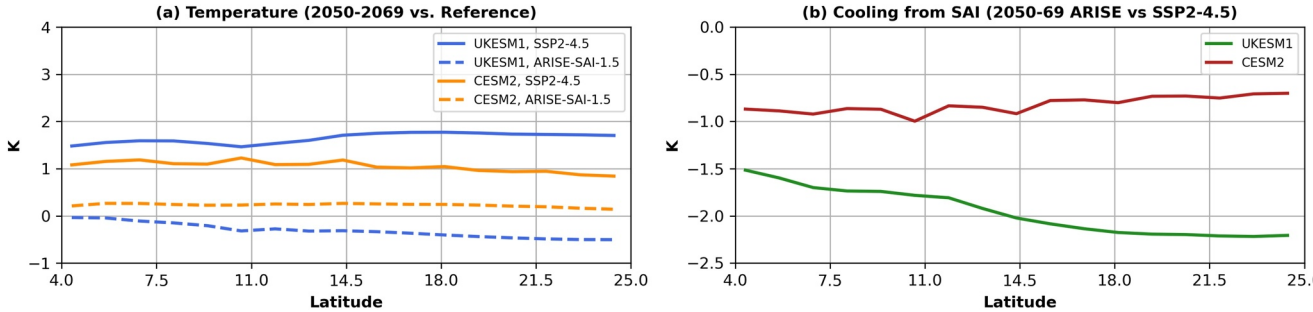

Figure 7. Comparison of (a) zonal-mean surface temperature change for UKESM1 and CESM2 and for SSP2-4.5 and ARISE-SAI-1.5 during the 2050–2069 period relative to the mean of the reference period (2015–2034). (b) The corresponding cooling from SAI.

uncertain, suggesting no clear difference between the internal climate variability and the forced response, whereas CESM2 (Figure 6b) exhibits isolated zones of statistically significant drying, mainly in the Sahel.

Under the ARISE-SAI-1.5 geoengineering scenario (Figures 6c and 6d), spatial patterns of SNR remain complex and heterogeneous. UKESM1 (Figure 6c) suggests patches of weak drying and wetting signals across West Africa, with statistically significant changes concentrated in localized coastal and north-western regions. CESM2 (Figure 6d) shows more extensive areas of significant positive SNR values, suggesting a slight shift toward wetter conditions in parts of the Sahel. However, the magnitude of these changes remains modest, and large portions of the region have stippling, indicating that precipitation anomalies under SAI are not statistically distinguishable from natural variability in most areas. These findings are consistent with previous studies highlighting how SAI could introduce additional complexities in precipitation projections by altering regional moisture transport and atmospheric circulation (Kravitz et al., 2017; Tilmes et al., 2018). The contrast between CESM2 and UKESM1 highlights structural differences in how the models simulate precipitation responses to SAI.

In light of these uncertainties, precipitation-related adaptation policies must be designed with high flexibility. Strategies such as improving water storage infrastructure, enhancing drought and flood resilience in agriculture, and investing in dynamic climate monitoring and early warning systems are crucial for safeguarding livelihoods against both wetter and drier future scenarios. Given the limited statistical robustness of projected precipitation changes, decision-making should prioritize resilience building and adaptive management rather than relying on specific rainfall projections.

3.4. Regional Precipitation and Temperature Differences by Latitude

Figure 7 presents a comparison of zonal-mean surface temperature changes across different latitudes in West Africa for the 2050–2069 period. We contrast the SSP2-4.5 and ARISE-SAI-1.5 scenarios for the UKESM1 and CESM2 climate models. In the SSP2-4.5 scenario (Figure 7a), both models indicate positive temperature anomalies across the examined latitudes, signifying warming relative to the reference period. UKESM1 projects higher temperature increases, remaining around 1.8 K throughout the region, while CESM2 shows a slightly lower warming trend, with values between 1 and 1.2 K. This discrepancy aligns with known differences in model sensitivities; CESM2 has been found to exhibit relatively lower climate sensitivity compared to UKESM1 in certain scenarios (Monerie et al., 2020; Pendergrass, 2020).

Under the ARISE-SAI-1.5 scenario (dashed lines), both models demonstrate reduced warming compared to SSP2-4.5, though with markedly different magnitudes. UKESM1 exhibits a pronounced cooling effect, with temperatures approaching or slightly dropping below 0 K relative to the reference period, while CESM2 shows a more moderate cooling impact, maintaining temperature changes between 0 and 0.3 K above the reference period. This distinct difference in response suggests that UKESM1 is more sensitive to SAI interventions, which is consistent with literature indicating varying responses among models to geoengineering due to differences in aerosol-cloud interaction representations (Fasullo & Richter, 2023; Henry et al., 2023).

Figure 7b quantifies the cooling effect of SAI by comparing temperature differences between the SSP2-4.5 and ARISE-SAI-1.5 scenarios across latitudes. Here, the UKESM1 model consistently demonstrates a more pronounced cooling response than CESM2 across all latitudes, with cooling intensifying at higher latitudes (up to

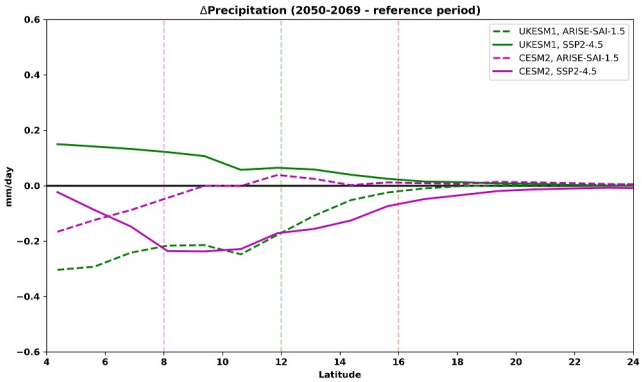

Figure 8. Comparison of zonal-mean precipitation change for UKESM1 and CESM2 and for SSP2-4.5 and ARISE-SAI-1.5 during the 2050–2069 period relative to the mean of the reference period (2015–2034).

−2.2 K in UKESM1 vs. a fairly uniform 1.0 K in CESM2). Although this latitudinal gradient in cooling suggests enhanced aerosol dispersal and differences in radiative forcing effectiveness between models (Tilmes et al., 2015), it may also reflect the differences influenced by the amounts and locations of SO_2 injected (Henry et al., 2023). Richter et al. (2022) show that CESM2 has the highest SO_2 loading around 15°S and much less near 30°N, likely due to the North Atlantic warming hole. In contrast, UKESM1 uses a more balanced injection pattern and reaches 1.5°C of warming earlier than CESM2. These timing and injection differences make direct comparisons between the models challenging. As Brody et al. (2024) point out, CESM2's response under ARISE-SAI-1.0 is more similar to UKESM1 under ARISE-SAI-1.5, highlighting the need to consider both the baseline climate and injection setup when comparing results.

The zonal mean changes in precipitation across different latitudes in West Africa reveal distinct responses in the UKESM1 and CESM2 under the SSP2-4.5 and ARISE-SAI-1.5 scenarios (Figure 8). UKESM1 projections under SSP2-4.5 show a moderate reduction in precipitation, though levels remain higher than the reference period levels across all latitudes, indicating a drying trend due to greenhouse gas emissions (Akinsanola et al., 2020). However, under the ARISE-SAI-1.5 scenario, UKESM1 exhibits more distinct regional variations in the precipitation response, with the Guinea Coast and Inland regions (approximately 4°N to 12°N) experiencing more severe drying conditions, while the Sahel region (around 12°N to 16°N) maintains precipitation levels closer to the baseline conditions. This aligns with Henry et al. (2024), who found that aerosol injections at 15°N and 30°N reduce equatorial precipitation more than subtropical precipitation, leading to differential drying effects across latitudes. The stabilization of Sahelian precipitation in UKESM1 suggests that SAI moderates the drying effects of climate change in semiarid regions while exacerbating water stress along the Guinea Coast.

Conversely, CESM2 shows a distinctly different precipitation response, exhibiting a more pronounced reduction under the SSP2-4.5 scenario, particularly in the Guinea Coast, where precipitation falls below reference period levels, indicating higher sensitivity to climate change compared to UKESM1. This response aligns with Zhang et al. (2024), who found that CESM2 requires higher aerosol injection rates to achieve the same cooling as UKESM1, leading to stronger precipitation suppression at lower latitudes. The stronger drying effect in CESM2 extends from the Guinea Coast into Inland West Africa and the Sahel, suggesting that the model simulates a more significant weakening of the West African monsoon due to climate change. Brody et al. (2024) show a similar response for CESM2 cooling to 1.0°C as UKESM cooling to 1.5°C. Under ARISE-SAI-1.5, CESM2 shows partial stabilization of rainfall near the Sahel (around 10°N to 15°N), but persistent drying continues in the Guinea Coast and Inland regions (4°N to 10°N), reinforcing Henry et al.'s (2024) findings that aerosol injection reduces equatorial convection more effectively than subtropical precipitation. These contrasting precipitation responses between UKESM1 and CESM2 underscore the complexity of regional climate projections in West Africa and the importance of intermodel comparisons in SAI research. Although both models agree on a general drying trend in the Guinea Coast and relative stabilization in the Sahel under ARISE-SAI-1.5, the intensity and spatial extent of drying differ significantly. UKESM1 projects a more moderate response, with precipitation reductions concentrated in the Guinea Coast but tapering off further north, maintaining near-reference period conditions in the Sahel. In contrast, CESM2 shows stronger suppression of rainfall at lower latitudes, consistent with findings by Zhang et al. (2024) and Bednarz et al. (2022, 2023), which link CESM2's enhanced precipitation sensitivity to its stratospheric aerosol transport characteristics and injection latitude effects on tropical convection.

These intermodel differences in precipitation response can be attributed to how each model's cloud microphysics and convective processes respond to aerosol-induced cooling. UKESM1's stronger drying along the Guinea Coast suggests that its convection scheme is more strongly stabilized under SAI (suppressing rainfall), whereas CESM2's precipitation, while also reduced, shows a slightly more uniform response with latitude. This is consistent with prior studies of SRM impacts on African monsoons—for example, Da-Allada et al. (2020) found that a stratospheric aerosol injection could overcorrect rainfall in coastal West Africa while maintaining Sahel precipitation due to weakened monsoon circulation. Similarly, Pinto et al. (2020) observed model-dependent hydrological responses over Africa under SAI, with some models showing significant precipitation reductions in West and Central Africa. Our results reflect these findings: UKESM1's aerosol-cloud interactions likely

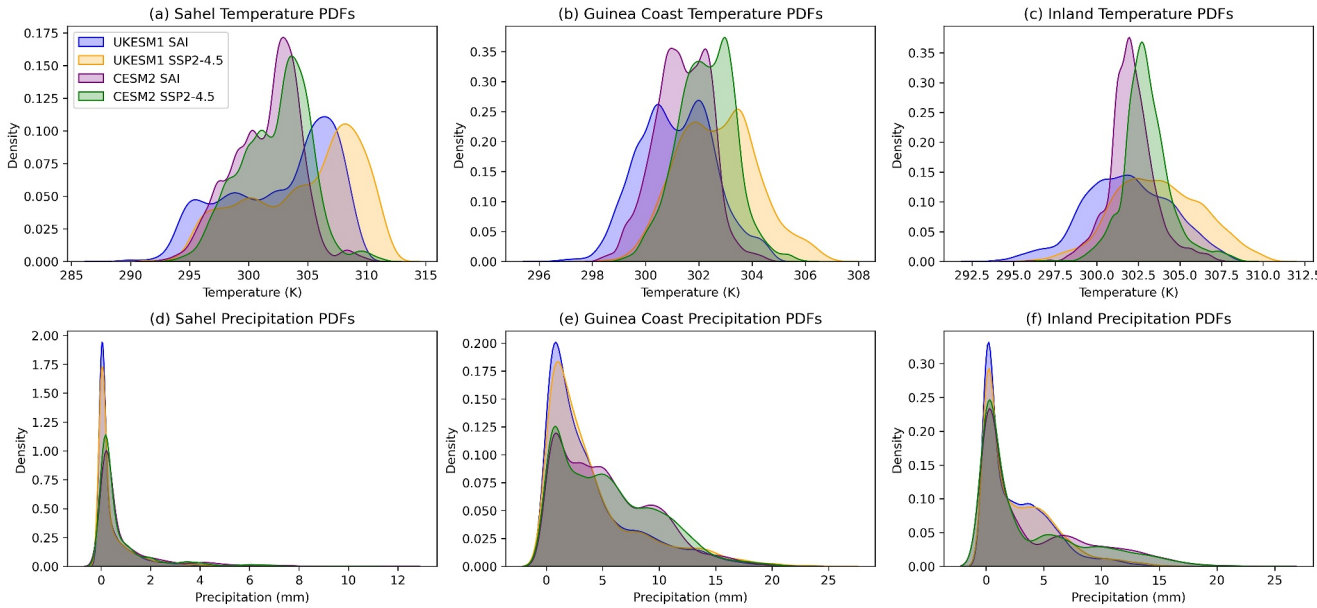

Figure 9. Comparison of probability density functions (PDFs) for temperature (a–c) and precipitation (d–f) under ARISE-SAI-1.5 and SSP2-4.5 scenarios across West African regions (Sahel, Guinea Coast, Inland).

amplify the suppression of convective rainfall, whereas CESM2's more moderate changes point to differences in feedbacks.

Our finding that SAI does not fully restore West African precipitation to baseline levels is consistent with Da-Allada et al. (2020), who found minimal net change in West African summer monsoon rainfall under a similar SAI experiment. Furthermore, the shifts in extreme precipitation we note align with the changes in precipitation indices reported by Tye et al. (2022) using GLENS simulations, which showed regionally varying impacts on heavy rainfall events. Notably, Abiodun et al. (2021) found that an SAI level sufficient to offset temperature increases could overcompensate and reduce precipitation in the tropics, leading to a net water deficit. Our results similarly indicate that while SAI cools the region, precipitation reductions in some areas mean it is not a panacea for hydrological stress. These findings are also in line with Liu et al. (2024), who highlighted the heterogeneous effects of SAI on tropical monsoons, with some subregions experiencing suppressed rainfall even as global temperatures are held in check.

The increased precipitation variability projected under SAI-1.5 in both models, though manifested differently, has important implications for agriculture and food security in West Africa. UKESM1 shows pronounced spatial heterogeneity, including intensified drying along the Guinea Coast, while CESM2 projects more subtle but still uncertain changes. In both models, this variability can disrupt planting and harvesting schedules in rain-fed agricultural systems, particularly in the Sahel and Guinea Savannah zones, where food production is tightly coupled to seasonal rainfall. Fluctuations in the onset and cessation of the rainy season, as well as the frequency of dry spells or heavy rain events, can lead to lower yields and increased risk of crop failure. These concerns are supported by past regional studies (Fosu-Mensah, MacCarthy et al., 2012; Fosu-Mensah, Vlek et al., 2012; Sultan et al., 2019), and highlight that while SAI may cool regional temperatures, its uncertain impact on precipitation reliability may compromise food and water security.

3.5. Probability Density Functions (PDFs) for Temperature and Precipitation

To further evaluate the shifts in climate extremes, Figure 9 presents the probability density functions (PDFs) of monthly precipitation under each scenario and model. The temperature analysis across West African regions reveals distinct patterns between the UKESM1 and CESM2 climate projections (Figure 9). In the Sahel region (Figure 9a), both models project warming trends under the SSP2-4.5 scenario, with CESM2 indicating slightly higher temperatures. However, when simulating the ARISE-SAI-1.5 scenario, the models diverge significantly: UKESM1 projects a dramatic cooling effect, showing substantially lower temperatures compared to SSP2-4.5,

while CESM2 demonstrates a more moderate temperature reduction, which, as noted earlier, could be attributed to the sensitivity to the timing of deployment.

Similar model differences emerge in the Guinea Coast and Inland regions, where CESM2 consistently projects warmer temperatures than UKESM1 under both scenarios (Figures 9b and 9c). Although both models show that SAI interventions lead to cooling across all areas, UKESM1 again demonstrates a more pronounced cooling effect. This consistent pattern of UKESM1 showing stronger responses to geoengineering interventions suggests fundamental differences in how these models simulate climate sensitivity to aerosol forcing.

The temperature PDFs highlight the more substantial cooling effects of SAI in UKESM1, suggesting this model is more sensitive to the cooling influence of stratospheric aerosol injection. CESM2 shows a less dramatic response to ARISE-SAI-1.5, maintaining higher temperatures in all regions compared to UKESM1. These differences in the temperature response between the two models may have important implications for future climate regulation strategies in West Africa, as the more varied temperature distribution in UKESM1 under geoengineering could present challenges for temperature management in the region.

The precipitation patterns across the regions show that while ARISE-SAI-1.5 has a significant impact on temperatures, its effects on precipitation are more regionally varied. In the Sahel and Inland regions (Figures 9d and 9f), the precipitation distributions are relatively similar across both models and scenarios, with most values concentrated below 4 mm/day. This suggests that precipitation changes under ARISE-SAI-1.5 are relatively minimal and consistent between UKESM1 and CESM2 in these areas.

In contrast, the Guinea Coast exhibits greater precipitation variability, with UKESM1 under ARISE-SAI-1.5 showing a higher peak indicating increased precipitation compared to SSP2-4.5 (Figure 9e). CESM2, on the other hand, shows a more gradual distribution with slightly lower precipitation under ARISE-SAI-1.5. This implies that the precipitation response to warming and geoengineering could be more complex in the Guinea Coast region, with the two models diverging in their simulations.

As shown in Figure 9, the PDFs of monthly precipitation under ARISE-SAI-1.5 and SSP2-4.5 are largely overlapping, especially for CESM2, indicating that SAI has minimal impact on shifting the central tendency of precipitation. This suggests that while temperature distributions shift clearly under SAI, precipitation shows far less response, reinforcing the conclusion that SAI is less effective in restoring hydrological conditions. This negative result is particularly relevant for water resource management in regions like the Sahel.

Overall, the precipitation distributions suggest that while SAI could significantly alter temperatures, particularly in the UKESM1 model, its impacts on precipitation are more regionally dependent. The Sahel and Inland regions show relatively consistent precipitation patterns across models and scenarios, while the Guinea Coast displays greater variability in the precipitation response to geoengineering interventions.

3.6. Cumulative Distribution Functions (CDFs) for Temperature and Precipitation

The analysis of the temperature CDFs reveals that geoengineering through ARISE-SAI-1.5 significantly reduces temperatures across all regions compared to the SSP2-4.5 scenario. This cooling effect is more pronounced in the UKESM1 model compared to CESM2, indicating that UKESM1 is more sensitive to the impacts of stratospheric aerosol injection. In the Sahel and Inland regions (Figures 10a and 10c), UKESM1 under ARISE-SAI-1.5 shows a more substantial shift toward cooler temperatures, with a steeper rise in the CDF around critical thresholds like 302 K in the Guinea Coast (Figure 10b). This suggests that geoengineering could be particularly effective at reducing the likelihood of extreme heat events in these regions, according to the UKESM1 model, which is attributable to differences in the models mentioned earlier.

In contrast, the precipitation CDFs show less consistent changes under the ARISE-SAI-1.5 scenario. All regions exhibit limited signs of drying (Figures 10d–10f), especially in the upper tail of the distribution, in UKESM1 under ARISE-SAI-1.5. CESM2, on the other hand, shows much smaller precipitation changes across both scenarios and regions, indicating that the geoengineering impacts on precipitation are more limited in this model. Notably, the direction of change varies by region, with CESM2 projecting drying over the Guinea Coast and wetting in the Sahel and Inland regions under ARISE-SAI-1.5.

The differences between the two models highlight how their representations of the impacts of SAI are different. UKESM1 consistently predicts greater changes in both temperature and precipitation under ARISE-SAI-1.5

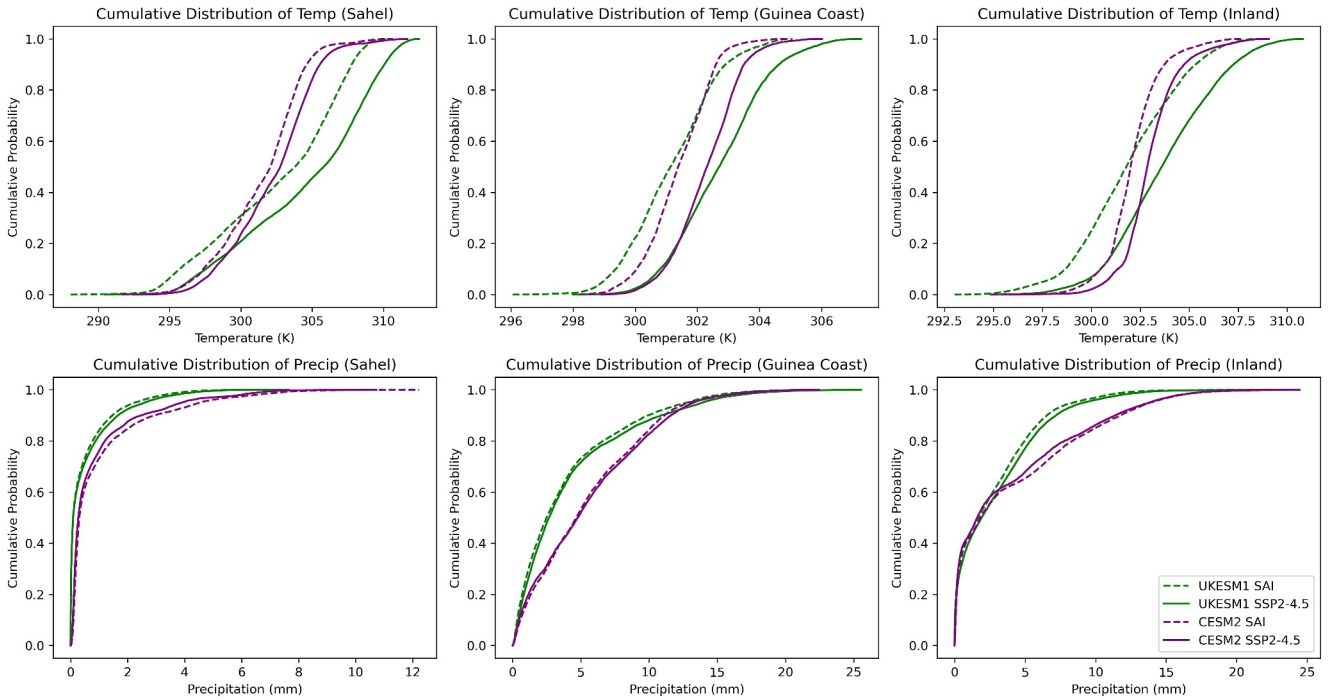

Figure 10. Comparison of cumulative distribution functions (CDFs) for temperature (a–c) and precipitation (d–f) under ARISE-SAI-1.5 and SSP2-4.5 scenarios across West African regions (Sahel, Guinea Coast, Inland).

compared to CESM2, which has a more muted response, particularly for precipitation. This divergence in model behavior could stem from fundamental differences in how they simulate aerosol-cloud interactions, feedback processes, or other internal model dynamics that govern the regional climate response to stratospheric aerosol injection.

4. Summary and Conclusion

This study provides a comprehensive analysis of regional climate trends in West Africa, focusing on the impacts of stratospheric aerosol injection (SAI) using two prominent climate models: the UK Earth System Model (UKESM1) and the Community Earth System Model version 2 (CESM2). Given West Africa's vulnerability to climate change, characterized by rising temperatures and shifting precipitation patterns, this research is crucial for understanding potential climate interventions. Utilizing the Shared Socioeconomic Pathway 2–4.5 (SSP2-4.5) as a baseline, the study projects climate scenarios for 2050–2069. The research methodology includes the evaluation of temperature and precipitation anomalies, signal-to-noise ratio (SNR) analysis to assess climate signal reliability, and cumulative distribution function (CDF) and probability density function (PDF) analyses to evaluate shifts in precipitation patterns.

The study reveals distinct warming patterns across West Africa under the SSP2-4.5 scenario, with notable differences between the two climate models. Specifically, UKESM1 predicts temperature increases up to 2.4°C, while CESM2 projects more moderate warming ranging from 1.8°C to 2.0°C. Under the ARISE-SAI-1.5 scenario, SAI produces somewhat contrasting effects: UKESM1 exhibits more pronounced cooling effects with temperature reductions reaching nearly −1.4°C in some areas, whereas CESM2 shows more moderate cooling effects, maintaining temperatures between 0°C and 0.5°C above the reference period. This suggests that UKESM1 may be more responsive to SAI interventions than CESM2. Differences in how the temperature target was chosen in UKESM also play a role, as explained in Henry et al. (2023), highlighting how it is important to further standardize SAI experiments to understand the projected outcomes, as discussed also in Visioni et al. (2024).

Further analyses provide deeper insights into these climate responses. The SNR analysis reveals that future temperature changes over West Africa are robust and statistically significant, emerging clearly above natural

variability by midcentury. In contrast, precipitation responses exhibit lower SNR values and greater spatial uncertainty, indicating weaker and less predictable hydrological changes. Additionally, CDF and PDF analyses reveal complex shifts in precipitation extremes under SAI. For instance, UKESM1 indicates that reductions in temperature due to SAI correlate with declines in precipitation, particularly during larger negative temperature anomalies. In contrast, CESM2 exhibits a more scattered relationship between temperature and precipitation changes under SAI.

The differences in model responses can be attributed to several underlying characteristics, including differences in the SAI injection strategy, such as injection altitude, latitude bands, and stratospheric aerosol distribution used by each model (Henry et al., 2023). UKESM1 incorporates interactive chemistry and robust aerosol-cloud interactions that amplify its response to SAI interventions (Lohmann & Feichter, 2005). Conversely, CESM2 employs a different injection setup (e.g., narrower latitude range and alternative vertical distribution), leading to more complex aerosol-cloud interactions and generally weaker radiative forcing comparable conditions (Davis & Medeiros, 2024; Gettelman et al., 2019).

It is important to note that precipitation responses under SAI do not fully return to baseline conditions, and in some cases, they may introduce new patterns of variability. The differences between UKESM1 and CESM2 highlight both structural and epistemic uncertainties, emphasizing the need for multimodel comparisons to better constrain precipitation responses to SAI. Furthermore, climate models operate at relatively coarse resolutions, which poses limitations in capturing convective rainfall processes—a dominant driver of precipitation in West Africa.

Overall, these findings highlight that while both models simulate reduced warming under the ARISE-SAI-1.5 scenario, they differ significantly in their projected outcomes, with UKESM1 projecting a more substantial cooling effect than CESM2. This variation between models in simulating projected reduced warming highlights a critical consideration in climate intervention assessment: the choice of model can significantly influence projected outcomes and, consequently, our understanding of potential climate risks and benefits. Such model-dependent variations emphasize the necessity of using multiple climate models when evaluating geoengineering strategies and their potential impacts on regional climate patterns rather than relying on single-model projections. Recent studies within the GeoMIP framework have emphasized the significance of multimodel comparisons in evaluating the effects of stratospheric aerosol injection (SAI). For instance, Visioni et al. (2021) demonstrated that while models generally agree on the global mean temperature response to SAI, they show considerable differences in regional climate impacts, particularly in precipitation patterns. Furthermore, Visioni et al. (2023) highlighted that multimodel analyses are crucial for assessing the potential side effects of SAI, such as changes in ozone concentrations and stratospheric dynamics, which can vary significantly between models.

These discrepancies in model predictions are critical for policy-making and adaptation strategies in West Africa. For example, if one were to rely solely on UKESM1's projection of substantial cooling and moderated rainfall under SAI, it could encourage optimistic interventions; however, CESM2's more modest cooling and continued dry tendencies urge caution. Our findings, therefore, carry a cautionary message: policy decisions around SAI deployment must account for significant model uncertainty. We stress that any hypothetical use of SAI to benefit West Africa's climate should be approached with extreme caution and always in parallel with traditional mitigation and adaptation efforts.

In practical terms, the projected changes in temperature and precipitation have direct implications for agriculture and water resources in West Africa. A cooler, drier outcome (as hinted by UKESM1 in the coastal regions) could lessen heat stress on crops but also reduce rainfall for rain-fed agriculture, potentially diminishing crop yields and straining irrigation and drinking water supplies. Conversely, a milder climate modification (as in CESM2) might mean fewer negative side effects but also less alleviation of warming. These socioeconomic impacts underscore the importance of interpreting our model results with caution. We have limited confidence in any single-model outcome; thus, robust decisions should be informed by a range of models and scenarios. Ultimately, our study highlights that geoengineering is not a guaranteed solution and its regional effects could be double-edged, offering some relief from warming while introducing new uncertainties in rainfall that communities and decision-makers would need to manage.

In conclusion, this study emphasizes the need for ongoing research into the implications of geoengineering strategies, such as SAI, on regional climate resilience in West Africa. This research highlights the need for further

investigation into optimal locations of stratospheric aerosol injection to offset climate change impacts while minimizing adverse effects on precipitation patterns in West Africa. Considering a range of climate model outputs is critical for developing effective adaptation strategies tailored to local conditions. The insights from this study can inform policymakers about the potential benefits and risks of geoengineering approaches in vulnerable regions. For policymakers, these results suggest that even under solar geoengineering, climate risk remains, particularly in the form of altered or unstable precipitation patterns. Governments should therefore prioritize adaptive planning that includes investment in climate-resilient agriculture, improved seasonal forecasting, and enhanced water resource infrastructure. Given the potential spatial variability in SAI outcomes, regional collaboration and monitoring will also be essential to ameliorate unintended effects and ensure equity in risk distribution. Further investigations into alternative injection materials and deployment strategies, including variations in latitude, altitude, and injection rates, could refine our understanding of regional climate impacts and optimize SAI design for minimal side effects. Finally, although the potential of SAI to reduce regional warming is notable, its implementation raises critical ethical and governance concerns. West Africa contributes minimally to global greenhouse gas emissions, yet stands to experience significant effects, both positive and negative, from any SAI deployment. Decisions about its use must therefore include voices from vulnerable regions, with equitable participation in scenario planning, risk assessments, and policy design. Without robust international governance, there is a risk of unequal burden-sharing or unintended regional impacts.

Conflict of Interest

The authors declare no conflicts of interest relevant to this study.

Data Availability Statement

Data sets used in this research are publicly available. The data for the UKESM model SSP2-4.5 simulations are available on the Earth System Grid Federation database, and the data for the SAI simulations are available at https://doi.org/10.5281/zenodo.11281900 (Henry, 2024). The ARISE-SAI and SSP2-4.5 data sets are additionally available for free download through the Amazon/AWS Open Data program. These can be accessed at https://registry.opendata.aws/ncar-cesm2-arise/ (Richter & Visioni, 2022a, 2022b).

Acknowledgments
We acknowledge the financial support of the DEGREES Modeling Fund (DMF) of the DEGREES Initiative. Kwesi A. Quagraine is supported by the National Science Foundation (NSF) National Center for Atmospheric Research (NCAR), a major facility sponsored by the U.S. NSF under Cooperative Agreement No. 1852977.

References

Abiodun, B. J., Odoulami, R. C., Sawadogo, W., Oloniyo, O. A., Abatan, A. A., New, M., et al. (2021). Potential impacts of stratospheric aerosol injection on drought risk managements over major river basins in Africa. *Climatic Change*, *169*(3–4), 31. https://doi.org/10.1007/s10584-021-03268-w

Ahmed, K. F., Wang, G., Yu, M., Koo, J., & You, L. (2015). Potential impact of climate change on cereal crop yield in West Africa. *Climatic Change*, *133*(2), 321–334. https://doi.org/10.1007/s10584-015-1462-7

Akinsanola, A. A., Zhou, W., Zhou, T., & Keenlyside, N. (2020). Amplification of synoptic to annual variability of West African summer monsoon rainfall under global warming. *Npj Climate and Atmospheric Science*, *3*(1), 21. https://doi.org/10.1038/s41612-020-0125-1

Akumaga, U., & Tarhule, A. (2018). Projected changes in intra-season rainfall characteristics in the Niger river Basin, West Africa. *Atmosphere*, *9*(12), 497. https://doi.org/10.3390/atmos9120497

Atiah, W. A., Muthoni, F. K., Kotu, B., Kizito, F., & Amekudzi, L. K. (2021). Trends of rainfall onset, cessation, and length of growing season in northern Ghana: Comparing the rain gauge, satellite, and farmer's perceptions. *Atmosphere*, *12*(12), 1674. https://doi.org/10.3390/atmos12121674

Bednarz, E. M., Visioni, D., Kravitz, B., Jones, A., Haywood, J. M., Richter, J., et al. (2023). Climate response to off-equatorial stratospheric Sulfur injections in three Earth System Models—Part 2: Stratospheric and free-tropospheric response. *Atmospheric Chemistry and Physics*, *23*(1), 663–685. https://doi.org/10.5194/acp-23-663-2023

Bednarz, E. M., Visioni, D., Richter, J. H., Butler, A. H., & MacMartin, D. G. (2022). Impact of the latitude of stratospheric aerosol injection on the southern Annular mode. *Geophysical Research Letters*, *49*(19). https://doi.org/10.1029/2022GL100353

Brody, E., Visioni, D., Bednarz, E. M., Kravitz, B., MacMartin, D. G., Richter, J. H., & Tye, M. R. (2024). Kicking the can down the road: Understanding the effects of delaying the deployment of stratospheric aerosol injection. *Environmental Research: Climate*, *3*(3), 035011. https://doi.org/10.1088/2752-5295/ad53f3

Carr, T. W., Mkuhlani, S., Segnon, A. C., Ali, Z., Zougmoré, R., Dangour, A. D., et al. (2022). Climate change impacts and adaptation strategies for crops in West Africa: A systematic review. *Environmental Research Letters*, *17*(5), 053001. https://doi.org/10.1088/1748-9326/ac61c8

Da-Allada, C. Y., Baloïtcha, E., Alamou, E. A., Awo, F. M., Bonou, F., Pomalegni, Y., et al. (2020). Changes in West African summer monsoon precipitation under stratospheric aerosol geoengineering. *Earth's Future*, *8*(7), e2020EF001595. https://doi.org/10.1029/2020ef001595

Danabasoglu, G., Lamarque, J. F., Bacmeister, J., Bailey, D. A., DuVivier, A. K., Edwards, J., et al. (2020). The Community Earth System Model version 2 (CESM2). *Journal of Advances in Modeling Earth Systems*, *12*(2), e2019MS001916. https://doi.org/10.1029/2019ms001916

Davis, I., & Medeiros, B. (2024). Assessing CESM2 clouds and their response to climate change using cloud regimes. *Journal of Climate*, *37*(10), 2965–2985. https://doi.org/10.1175/JCLI-D-23-0337.1

Fao, F. A. O. S. T. A. T. (2018). *Food and Agriculture Organization of the United Nations*. 403. http://faostat.fao.org

Fasullo, J. T., & Richter, J. H. (2023). Dependence of strategic solar climate intervention on background scenario and model physics. *Atmospheric Chemistry and Physics*, *23*(1), 163–182. https://doi.org/10.5194/acp-23-163-2023

Fosu-Mensah, B. Y., MacCarthy, D. S., Vlek, P. L. G., & Safo, E. Y. (2012a). Simulating impact of seasonal climatic variation on the response of maize (Zea Mays L.) to inorganic fertilizer in sub-humid Ghana. *Nutrient Cycling in Agroecosystems*, *94*(2–3), 255–271. https://doi.org/10.1007/s10705-012-9539-4

Fosu-Mensah, B. Y., Vlek, P. L., & MacCarthy, D. S. (2012). Farmers' perception and adaptation to climate change: A case study of Sekyedumase district in Ghana. *Environment, Development and Sustainability*, *14*(4), 495–505. https://doi.org/10.1007/s10668-012-9339-7

Fraumeni, B. M., & Liu, G. (2021). Summary of world economic forum. In *Measuring human capital* (pp. 125–138). Academic Press. The Global Human Capital Report 2017—Preparing people for the future of work. https://doi.org/10.1016/B978-0-12-819057-9.00008-1

Gettelman, A., Hannay, C., Bacmeister, J. T., Neale, R. B., Pendergrass, A. G., Danabasoglu, G., et al. (2019). High climate sensitivity in the Community Earth System Model version 2 (CESM2). *Geophysical Research Letters*, *46*(14), 8329–8337. https://doi.org/10.1029/2019GL083978

Hawkins, E., & Sutton, R. (2009). Decadal predictability of the Atlantic Ocean in a coupled GCM: Forecast skill and optimal perturbations using linear inverse modeling. *Journal of Climate*, *22*(14), 3960–3978. https://doi.org/10.1175/2009jcli2720.1

Henry, M. (2024). Data for "how does the latitude of stratospheric Aerosol injection affect the climate in UKESM1? [Dataset]. *Zenodo*. https://doi.org/10.5281/zenodo.11281900

Henry, M., Bednarz, E. M., & Haywood, J. (2024). How does the latitude of stratospheric aerosol injection affect the climate in UKESM1? *Atmospheric Chemistry and Physics*, *24*(23), 13253–13268. https://doi.org/10.5194/acp-24-13253-2024

Henry, M., Haywood, J., Jones, A., Dalvi, M., Wells, A., Visioni, D., et al. (2023). Comparison of UKESM1 and CESM2 simulations using the same multi-target stratospheric aerosol injection strategy. *Atmospheric Chemistry and Physics*, *23*(20), 13369–13385. https://doi.org/10.5194/acp-23-13369-2023

IPCC. (2021). In V. Masson-Delmotte, P. Zhai, A. Pirani, S. L. Connors, C. Péan, et al. (Eds.), *Climate change 2021: The physical science basis. Contribution of working group I to the Sixth assessment report of the intergovernmental panel on climate change*. Cambridge University Press. https://doi.org/10.1017/9781009157896

Irvine, P., Emanuel, K., He, J., Horowitz, L. W., Vecchi, G., & Keith, D. (2019). Halving warming with idealized solar geoengineering moderates key climate hazards. *Nature Climate Change*, *9*(4), 295–299. https://doi.org/10.1038/s41558-019-0398-8

Jones, A. C., Hawcroft, M. K., Haywood, J. M., Jones, A., Guo, X., & Moore, J. C. (2018). Regional climate impacts of stabilizing global warming at 1.5 K using solar geoengineering. *Earth's Future*, *6*(2), 230–251. https://doi.org/10.1002/2017ef000720

Klutse, N. A. B., Owusu, K., Nkrumah, F., & Anang, O. A. (2021). Projected rainfall changes and their implications for rainfed agriculture in northern Ghana. *Weather*, *76*(10), 340–347. https://doi.org/10.1002/wea.4015

Kravitz, B., MacMartin, D. G., Mills, M. J., Richter, J. H., Tilmes, S., Lamarque, J. F., et al. (2017). First simulations of designing stratospheric sulfate aerosol geoengineering to meet multiple simultaneous climate objectives. *Journal of Geophysical Research: Atmospheres*, *122*(23), 12–616. https://doi.org/10.1002/2017jd026874

Limantol, A. M., Larbi, I., Dotse, S. Q., Okafor, G. C., Asare-Nuamah, P., Frimpong, L. K., et al. (2023). An increase in temperature under the shared socioeconomic scenarios in the Volta river basin, West Africa: Implications for economic development. *Journal of Water and Climate Change*, *14*(8), 2808–2824. https://doi.org/10.2166/wcc.2023.141

Liu, Z., Lang, X., & Jiang, D. (2024). Stratospheric aerosol injection geoengineering would mitigate greenhouse gas-induced drying and affect global drought patterns. *Journal of Geophysical Research: Atmospheres*, *129*(3), e2023JD039988. https://doi.org/10.1029/2023jd039988

Lohmann, U., & Feichter, J. (2005). Global indirect aerosol effects: A review. *Atmospheric Chemistry and Physics*, *5*(3), 715–737. https://doi.org/10.5194/acp-5-715-2005

MacCarthy, D. S., Adam, M., Freduah, B. S., Fosu-Mensah, B. Y., Ampim, P. A., Ly, M., et al. (2021). Climate change impact and variability on cereal productivity among smallholder farmers under future production systems in West Africa. *Sustainability*, *13*(9), 5191. https://doi.org/10.3390/su13095191

MacMartin, D. G., Visioni, D., Kravitz, B., Richter, J. H., Felgenhauer, T., Lee, W. R., et al. (2022). Scenarios for modeling solar radiation modification. *Proceedings of the National Academy of Sciences*, *119*(33), e2202230119. https://doi.org/10.1073/pnas.2202230119

Monerie, P. A., Wainwright, C. M., Sidibe, M., & Akinsanola, A. A. (2020). Model uncertainties in climate change impacts on Sahel precipitation in ensembles of CMIP5 and CMIP6 simulations. *Climate Dynamics*, *55*(5), 1385–1401. https://doi.org/10.1007/s00382-020-05332-0

Muzammal, H., Zaman, M., Safdar, M., Adnan Shahid, M., Sabir, M. K., Khil, A., et al. (2024). Climate change impacts on water resources and implications for agricultural management. In *Transforming agricultural management for a sustainable future: Climate change and machine learning perspectives* (pp. 21–45). Springer Nature Switzerland. https://doi.org/10.1007/978-3-031-63430-7_2

Nicholson, S. E., Fink, A. H., & Funk, C. (2018). Assessing recovery and change in West Africa's rainfall regime from a 161-year record. *International Journal of Climatology*, *38*(10), 3770–3786. https://doi.org/10.1002/joc.5530

Niemeier, U., Richter, J. H., & Tilmes, S. (2020). Differing responses of the quasi-biennial oscillation to artificial SO_2 injections in two global models. *Atmospheric Chemistry and Physics*, *20*(14), 8975–8987. https://doi.org/10.5194/acp-20-8975-2020

Obahoundje, S., N'guessan Bi, V. H., Diedhiou, A., Kravitz, B., & Moore, J. C. (2022). Influence of stratospheric aerosol geoengineering on temperature mean and precipitation extremes indices in Africa. *International Journal of Climate Change Strategies and Management*, *14*(4), 399–423. https://doi.org/10.1108/IJCCSM-03-2021-0028

O'Neill, B. C., Tebaldi, C., Van Vuuren, D. P., Eyring, V., Friedlingstein, P., Hurtt, G., et al. (2016). The Scenario Model Intercomparison Project (ScenarioMIP) for CMIP6. *Geoscientific Model Development*, *9*(9), 3461–3482. https://doi.org/10.5194/gmd-9-3461-2016

Onyeaka, H., Nwauzoma, U. M., Akinsemolu, A. A., Tamasiga, P., Duan, K., Al-Sharify, Z. T., & Siyanbola, K. F. (2024). The ripple effects of climate change on agricultural sustainability and food security in Africa. *Food and Energy Security*, *13*(5), e567. https://doi.org/10.1002/fes3.567

Patel, T. D., Odoulami, R. C., Pinto, I., Egbebiyi, T. S., Lennard, C., Abiodun, B. J., & New, M. (2023). Potential impact of stratospheric aerosol geoengineering on projected temperature and precipitation extremes in South Africa. *Environmental Research: Climate*, *2*(3), 035004. https://doi.org/10.1088/2752-5295/acdaec

Pendergrass, A. G. (2020). The global-mean precipitation response to CO_2-induced warming in CMIP6 models. *Geophysical Research Letters*, *47*(17), e2020GL089964. https://doi.org/10.1029/2020GL089964

Pinto, I., Jack, C., Lennard, C., Tilmes, S., & Odoulami, R. C. (2020). Africa's climate response to solar radiation management with stratospheric aerosol. *Geophysical Research Letters*, *47*(2), e2019GL086047. https://doi.org/10.1029/2019gl086047

Richter, J., & Visioni, D. (2022a). SSP2-4.5 simulations with CESM2 (WACCM6) [Dataset]. *Zenodo*. https://doi.org/10.5281/zenodo.6473954

Richter, J., & Visioni, D. (2022b). ARISE-SAI-1.5: Assessing responses and impacts of solar climate intervention on the earth system with stratospheric aerosol injection, with cooling to 1.5C [Dataset]. *Zenodo*. https://doi.org/10.5281/zenodo.6473775

Richter, J. H., Visioni, D., MacMartin, D. G., Bailey, D. A., Rosenbloom, N., Dobbins, B., et al. (2022). Assessing responses and impacts of solar climate intervention on the earth system with Stratospheric Aerosol Injection (ARISE-SAI): Protocol and initial results from the first simulations. *Geoscientific Model Development*, *15*(22), 8221–8243. https://doi.org/10.5194/gmd-15-8221-2022

Robock, A., Oman, L., & Stenchikov, G. L. (2008). Regional climate responses to geoengineering with tropical and Arctic SO_2 injections. *Journal of Geophysical Research*, *113*(D16). https://doi.org/10.1029/2008jd010050

Sellar, A. A., Jones, C. G., Mulcahy, J. P., Tang, Y., Yool, A., Wiltshire, A., et al. (2019). UKESM1: Description and evaluation of the UK earth system model. *Journal of Advances in Modeling Earth Systems*, *11*(12), 4513–4558. https://doi.org/10.1029/2019MS001739

Shindell, D., Parsons, L., Faluvegi, G., Hicks, K., Kuylenstierna, J., & Heaps, C. (2023). The important role of African emissions reductions in projected local rainfall changes. *npj Climate and Atmospheric Science*, *6*(1), 47. https://doi.org/10.1038/s41612-023-00382-7

Sivakumar, M. V. (2020). Climate extremes and impacts on agriculture. *Agroclimatology: Linking Agriculture to Climate*, *60*, 621–647. https://doi.org/10.2134/agronmonogr60.2016.0003

Smith, W., Bhattarai, U., Bingaman, D. C., Mace, J. L., & Rice, C. V. (2022). Review of possible very high-altitude platforms for stratospheric aerosol injection. *Environmental Research Communications*, *4*(3), 031002. https://doi.org/10.1088/2515-7620/ac4f5d

Sultan, B., Defrance, D., & Iizumi, T. (2019). Evidence of crop production losses in West Africa due to historical global warming in two crop models. *Scientific Reports*, *9*(1), 12834. https://doi.org/10.1038/s41598-019-49167-0

Sultan, B., & Gaetani, M. (2016). Agriculture in West Africa in the twenty-first century: Climate change and impacts scenarios, and potential for adaptation. *Frontiers in Plant Science*, *7*, 1262. https://doi.org/10.3389/fpls.2016.01262

Tebaldi, C., Debeire, K., Eyring, V., Fischer, E., Fyfe, J., Friedlingstein, P., et al. (2021). Climate model projections from the Scenario Model Intercomparison Project (ScenarioMIP) of CMIP6. *Earth System Dynamics*, *12*(1), 253–293. https://doi.org/10.5194/esd-12-253-2021

Tilmes, S., Fasullo, J., Lamarque, J. F., Marsh, D. R., Mills, M., Alterskjaer, K., et al. (2013). The hydrological impact of geoengineering in the Geoengineering Model Intercomparison Project (GeoMIP). *Journal of Geophysical Research: Atmospheres*, *118*(19), 11–036. https://doi.org/10.1002/jgrd.50868

Tilmes, S., Lamarque, J. F., Emmons, L. K., Kinnison, D. E., Ma, P. L., Liu, X., et al. (2015). Description and evaluation of tropospheric chemistry and aerosols in the Community Earth System Model (CESM1. 2). *Geoscientific Model Development*, *8*(5), 1395–1426. https://doi.org/10.5194/gmd-8-1395-2015

Tilmes, S., Richter, J. H., Kravitz, B., MacMartin, D. G., Mills, M. J., Simpson, I. R., et al. (2018). CESM1 (WACCM) stratospheric aerosol geoengineering large ensemble project. *Bulletin of the American Meteorological Society*, *99*(11), 2361–2371. https://doi.org/10.1175/BAMS-D-17-0267.1

Trenberth, K. E., & Shea, D. J. (2005). Relationships between precipitation and surface temperature. *Geophysical Research Letters*, *32*(14). https://doi.org/10.1029/2005GL022760

Tye, M. R., Dagon, K., Molina, M. J., Richter, J. H., Visioni, D., Kravitz, B., & Tilmes, S. (2022). Indices of Extremes: Geographic patterns of change in extremes and associated vegetation impacts under climate intervention. *Earth System Dynamics*, *13*(3), 1233–1257. https://doi.org/10.5194/esd-13-1233-2022

UNFCCC. (2015). Report on the structured expert dialogue on the 2013–2015 review. Retrieved From http://unfccc.int/resource/docs/2015/sb/eng/inf01.pdfUNFCCC. This document prepared in advance of the Paris Agreement provides the underlying rationale for setting changes in global temperature as climate targets

Visioni, D., Kravitz, B., Robock, A., Tilmes, S., Haywood, J. M., Boucher, O., et al. (2023). Opinion: The scientific and community-building roles of the Geoengineering Model Intercomparison Project (GeoMIP)-past, present, and future. *Atmospheric Chemistry and Physics Discussions*, *2023b*(9), 5149–5176. https://doi.org/10.5194/acp-23-5149-2023

Visioni, D., MacMartin, D. G., Kravitz, B., Boucher, O., Jones, A., Lurton, T., et al. (2021). Identifying the sources of uncertainty in climate model simulations of solar radiation modification with the G6sulfur and G6solar Geoengineering Model Intercomparison Project (GeoMIP) simulations. *Atmospheric Chemistry and Physics*, *21*(13), 10039–10063. https://doi.org/10.5194/acp-21-10039-2021

Visioni, D., Robock, A., Haywood, J., Henry, M., Tilmes, S., MacMartin, D. G., et al. (2024). G6-1.5 K-SAI: A new Geoengineering Model Intercomparison Project (GeoMIP) experiment integrating recent advances in solar radiation modification studies. *Geoscientific Model Development*, *17*(7), 2583–2596. https://doi.org/10.5194/gmd-17-2583-2024

Walters, D., Baran, A. J., Boutle, I., Brooks, M., Earnshaw, P., Edwards, J., et al. (2019). The Met Office Unified Model global atmosphere 7.0/7.1 and JULES global land 7.0 configurations. *Geoscientific Model Development*, *12*(5), 1909–1963. https://doi.org/10.5194/gmd-12-1909-2019

Zhang, Y., MacMartin, D. G., Visioni, D., Bednarz, E. M., & Kravitz, B. (2024). Hemispherically symmetric strategies for stratospheric aerosol injection. *Earth System Dynamics*, *15*(2), 191–213. https://doi.org/10.5194/esd-15-191-2024